Partial decay widths of resonances in ^{29}P†

N. Tsoupas, H. J. Hausman, N. L. Gearhart,* and G. H. Terry
Department of Physics, The Ohio State University, Columbus, Ohio 43210
(Received 30 July 1975)

Absolute differential cross sections of the ^{28}Si$(p,p')^{28}$Si* (1.78 MeV) reaction have been measured for 12 scattering angles and at 88 different energies between bombarding energies of 3.0 to 5.2 MeV. In addition, 53 absolute cross sections of the ^{28}Si$(p,p'\gamma)^{28}$Si angular correlations in the spin-flip geometry were also measured over the same energy region. From these and other data, the partial proton decay widths and phases of 14 resonances in ^{29}P were determined between excitation energies of 5.50 and 7.90 MeV.

[NUCLEAR REACTIONS ^{28}Si(p,p_1), measured $\sigma(E,\theta)$, $E=3.0-5.2$ MeV. ^{28}Si$(p,p_1\gamma)$, measured p-γ correlations in the spin-flip geometry, determined partial proton decay widths, Γ_{lj}, for 14 resonances. Calculated reduced widths.]

I. INTRODUCTION

In our continuing work investigating the properties of resonance states in ^{29}P, this paper reports on the determination of the decay parameters (partial decay widths and relative phases) of some of the resonance states in ^{29}P at excitation energies from 5.5 to 7.9 MeV. In a previous paper,[1] we reported on the determination of the spins of the resonances in this energy region utilizing proton–γ-ray angular-correlation measurements in the Goldfarb-Seyler[2] geometry. This current work involves measurements of detailed angular distributions of the inelastically scattered protons, the ^{28}Si$(p,p')^{28}$Si* (1.78 MeV first excited state) reaction, as well as proton–γ-ray angular correlations in the spin-flip geometry measured over the same energy region. The absolute cross sections determined from all three experiments were then utilized to extract the decay parameters of the resonances in ^{29}P.

The determination of the decay properties of the resonant states depends upon the measurement of a number of experimental quantities equal to or greater than the number of decay amplitudes and phases. As an example, consider the inelastic scattering of protons from a spin-zero target leading to a 2^+ final state via an isolated $J=5/2$ resonance. If the parity of the resonance is known, then there remains to determine five decay amplitudes (1/2, 3/2, 5/2, 7/2, and 9/2) and four relative phases (for an isolated resonance one phase is arbitrary). Consequently, for this example, a minimum of nine experimental quantities are required in order to unambiguously determine the possible nine amplitudes and phases. The angular correlation previously measured over the ^{29}P resonance measurements in the Goldfarb-Seyler geometry can be expressed as $W(\phi_\gamma,\theta_\gamma=\frac{1}{2}\pi)=\sum_{\kappa\ \mathrm{even}} A_\kappa \cos\kappa\phi_\gamma$. For a 5/2 resonance, only three coefficients, (and hence three experimental quantities) are determined. In order to specify all the decay parameters of this hypothetical isolated spin-5/2 resonance, at least six additional parameters must be determined from other experiments. We have chosen two additional experiments from which the six remaining parameters can be determined: the first is a measurement of the angular distribution of the inelastically scattered protons; the second is the proton–γ-ray angular correlations in the spin-flip geometry. Details of these geometries are described in Sec. II. Each of the additional experiments provides three experimental quantities for a total of nine, just sufficient to determine the nine resonance parameters. All the other resonance parameters such as total width, partial elastic proton width, spin, and parity of the resonance have previously been determined from elastic scattering experiments[3–5] and angular-correlation measurements in the Goldfarb-Seyler geometry.[1]

The experimental situation is improved by the fact that none of the resonances studied in this energy region is truly *isolated*. Every resonance experiences interference with neighboring resonances. Consequently the restriction that the expansion functions for the angular distributions and spin-flip correlations contain only even coefficients is relaxed. Interference between resonances of opposite parity induces odd coefficients in the expansion functions and hence provides additional experimental quantities for determining the resonance parameters. If we now consider as an example the interference between two spin-5/2 resonances of opposite parity, there are 10 parameters for each resonance to be determined; i.e., 5 amplitudes and 5 phases for a total of 20 possible parameters for the two resonances. However, the

additional odd coefficients now possible for the angular distributions and spin-flip correlations give rise to a total number of 26 possible experimental quantities and hence overdetermine the unknown resonance parameters.

The partial decay proton widths are related to the reduced widths through the penetrability factor. The physical meaning of the reduced width can be interpreted as the "degree" or probability amplitude in which a single particle is coupled to a core nucleus to form a new nucleus.[6] Therefore, such results can be used for comparison with the theoretical results derived from nuclear structure models which are based upon such core-particle couplings.

II. EXPERIMENTAL GEOMETRIES

In this section we show how the parameters under determination (partial decay widths and phases) appear in the theoretical expressions of the angular distributions and correlations for spin-1/2 particles on 0^+ targets.

In any reaction of the type $X(p, p', \gamma)X$ where an intermediate state with definite spin and parity is formed, the probability that we detect the outgoing radiations p', γ in the solid angles $d\Omega_{p'}, d\Omega_\gamma$ is given by[7]

$$\frac{d^2\sigma}{d\Omega_{p'} d\Omega_\gamma} = (\text{const})\lambda\!\!\!^{-2} \sum B(\alpha)\,\mathrm{Re}\left[Y^{\kappa_1 *}_{k_1}(\Omega_p) Y^{\kappa_2}_{k_2}(\Omega_{p'}) Y^{\kappa_3}_{k_3}(\Omega_\gamma)\right] \times \mathrm{Re}(\langle|\theta|\rangle\langle|\theta|\rangle^*), \quad (1)$$

where $\lambda\!\!\!^{-}$ is the reduced wavelength of the incident radiation, and B represents the products of angular momenta addition coefficients which depend upon the spin and parities of the target, compound, and residual nucleus as well as upon the angular momenta of the involved radiations. The summation is over all the quantum numbers involved.

The real part of the product of the three spherical harmonics describes the angular dependence of the radiations. This part depends upon the particular arrangements of the detectors with respect to a defined coordinate system. (We call such a type of an arrangement "a geometry".)

We assume that the type of interaction of the target nucleus with the incident particle is of Breit-Wigner form. Under this assumption the explicit expression of the product of the two matrix elements which appear in the above formula is given by

$$\langle|\theta|\rangle\langle|\theta|\rangle^* = \frac{(\Gamma_{b,j_1})^{1/2} e^{i\phi_{b,j_1}} (\Gamma_{b,j_2})^{1/2} e^{i\phi_{b,j_2}}}{(E - E_b) + i\frac{1}{2}\Gamma_b} \times \frac{(\Gamma_{b',j_1'})^{1/2} e^{-i\phi_{b',j_1'}} (\Gamma_{b',j_2'})^{1/2} e^{-i\phi_{b',j_1'}}}{(E - E_{b'}) - i\frac{1}{2}\Gamma_{b'}},$$

where E_b, Γ_b is the resonance energy and the total width of the resonance state with spin J_b; j_1 and j_2 are the total angular momenta of the incident and outgoing proton, respectively; and Γ_{b,j_1}, Γ_{b,j_2} are the partial widths for the formation and decay of the resonance state J_b, respectively. The prime quantities are referred to a nearby resonance state which interferes with b and ϕ_{b,j_1} and ϕ_{b,j_2} are the phases.

The experimentally measured quantities which depend upon the partial widths and phases are the expansion coefficients of the angular distributions and correlations. We consider each of the experimental geometries separately.

A. Inelastic proton angular distributions

The inelastic proton angular distribution in a coordinate system in which the z axis is chosen along the incident beam direction can be expanded in terms of Legendre polynomials as:

$$\frac{d\sigma}{d\Omega_{p'}} = \sum_{k=0}^{k_{\max}} A_k(E) P_k(\cos\theta), \quad (2)$$

where

$$k_{\max} = \min(l_1 + l_1', l_2 + l_2', j_2 + j_2', J_b + J_{b'})$$

and l_1 and l_2 are the orbital angular momentum of the incident or scattered proton, respectively. The coefficients $A_k(E)$ are functions of the partial widths and phases of the resonant state. Thus if we determine the coefficients A_k experimentally we provide information for the determination of the unknown parameters. The presence of odd coefficients in the angular distributions and spin-flip correlations adds significant information concerning the decay parameters. The odd coefficients can only occur when there is interference between states of opposite parity whereas the even coefficients contain both self-resonant contributions as well as contributions due to interference between states of the same parity.

B. Spin-flip correlation geometry

Additional information for the determination of these parameters is provided from the expansion coefficients of the angular correlation in the spin-flip geometry. In this geometry the z axis is defined perpendicular to the reaction plane

measurements involve the angular correlations between the inelastically scattered protons and the decay γ rays from the first excited 2^+ state in ^{28}Si. The probability of detecting a γ ray along the z axis in coincidence with an inelastically scattered proton at an angle $\phi_{p'}$ is given by

$$\frac{d^2\sigma}{d\Omega_{p'}d\Omega_\gamma}(\theta_{p'}=\tfrac{1}{2}\pi,\ \phi_{p'},\ \theta_\gamma=0)=\sum_{\kappa=0}^{\kappa_{\max}} C_\kappa(E)\cos(\kappa\phi_{p'})\,. \tag{3}$$

The restrictions on $\kappa_{\max}$ are the same as those for the proton angular distributions. As in the case of the proton angular distribution, both even and odd coefficients are possible, the odd coefficients resulting from any interference between resonant states of opposite parity.

C. Angular correlations in the Goldfarb-Seyler geometry

The last of the three experiments utilized to determine the resonant decay parameter was the angular correlation of the inelastically scattered protons and the decay γ rays from the first excited 2^+ state in ^{28}Si measured in the Goldfarb-Seyler geometry.[2] The z axis in this geometry is defined as being along the direction of the scattered proton; the coincident γ rays are then measured along the surface of a cone about that z axis. For data reported here, the proton detector angle was set at an angle of 90° c.m. with respect to the incident beam direction and the γ-ray detectors moved on the $\theta_\gamma=\frac{1}{2}\pi$ cone surface, i.e., in a plane perpendicular to the z axis.

The angular correlations can be expressed as

$$\frac{d^2\sigma}{d\Omega_{p'}d\Omega_\gamma}(\theta_\gamma=\tfrac{1}{2}\pi,\ \phi_\gamma,\ \theta_{p'}=0)=\sum_{\substack{\kappa=0\\ \text{even}}}^{\kappa_{\max}} D_k(E)\cos(\kappa\phi_\gamma)\,, \tag{4}$$

where $\kappa_{\max}\leq(L_3+L_3',\ l_1+l_1',\ J_b+J_{b'})$ and only the even terms in κ are permitted. The quantity L_3 (or L_3') refers to the γ-ray multipolarity of the emitted γ rays. For the present experiment $L_3+L_3'=4$. Unlike the cases for the proton angular distributions and spin-flip correlations, the complexity, κ of the Goldfarb-Seyler correlations is not limited by the l_2 value or j_2 value of the inelastic protons emitted from the compound nucleus. However, because of the particular γ detector cone angle of 90°, only even coefficients are allowed and hence we are unable to observe interference between resonances of opposite parity.

III. EXPERIMENTAL CONSIDERATIONS

The proton beam was provided by The Ohio State University 7 MV Van de Graaff accelerator. Targets were prepared by electron-beam evaporation of natural SiO_2 onto thin carbon foils. Although naturally occurring SiO_2 has an isotopic abundance of 92.2% ^{28}Si, the inelastic proton peak corresponding to decay to the first excited state in ^{28}Si was well separated from the proton groups from other target isotopes. Targets of different thicknesses were prepared for the angular distribution and angular-correlation experiments since the count-rate problems differed for the two different types of experiments.

The angular distributions of the inelastically scattered protons from the ^{28}Si first excited state were measured in a 43.2 cm Ortec scattering chamber. For these measurements the target thickness was measured as being 45 μg/cm^2. Target thicknesses were determined by comparison of the measured elastic scattering of protons at 2 MeV with the Coulomb cross section. There was no target deterioration measureable over the time of the experiments. Six silicon surface barrier detectors were used to detect the scattered protons. The base plate of the scattering chamber could be rotated so that two different angular positions of the base plate could provide information for 12 scattering angles. The proton bombarding energy was varied from 3.0 to 5.2 MeV and 88 angular distributions were measured over this energy region. Pileup-rejection electronics were used to correct the recorded spectra for pileup losses. An on-line 1800 computer was used to collect the spectra from the six proton detectors. The inelastic proton yields were converted to absolute cross sections with an over-all uncertainty of ±3%.

Five of these angular distributions, measured over the resonance at 3.33 MeV are shown in Fig. 1. The strong interference of this seemingly isolated resonance with neighboring resonances can be seen by the marked change in the shape of the distributions over the resonance. The solid curves shown in the figure are the least-squares fit to the data in terms of Legendre polynomials. The Legendre polynomial coefficients were extracted from the least-squares fit to the data and the energy variations of these coefficients were used in the partial width determinations.

The technique of measuring spin-flip correlations was first described and used by Schmidt *et al.*[8] Since that time this technique has proven to be very useful both for reaction-mechanism studies and for spectroscopic studies. The unique features of the spin-flip correlation measurements were not emphasized in the experiments reported here. The spin-flip measurements were chosen merely to increase the number of experimental quantities from which the decay widths could be determined, i.e., another experimental geometry. In the spin-flip

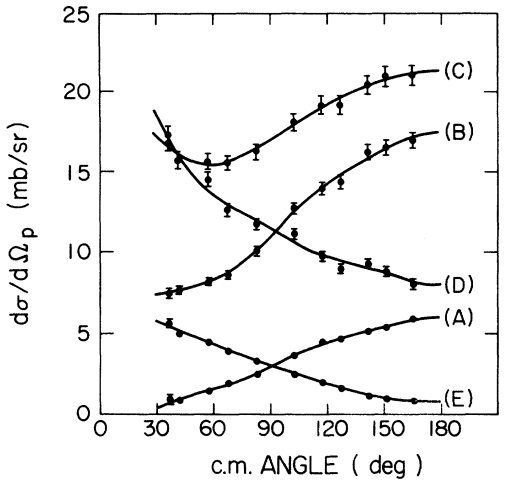

FIG. 1. The ^{28}Si$(p, p')^{28}$Si* (2^+, 1.78 MeV) inelastic angular distributions over the E_p=3.33 MeV resonance in ^{29}P. Curve A corresponds to a bombarding energy of 3.310 MeV; B to 3.325 MeV; C to 3.340 MeV; D to 3.350 MeV; and E to 3.365 MeV. The solid curve is a least-squares fit to the data, for each energy.

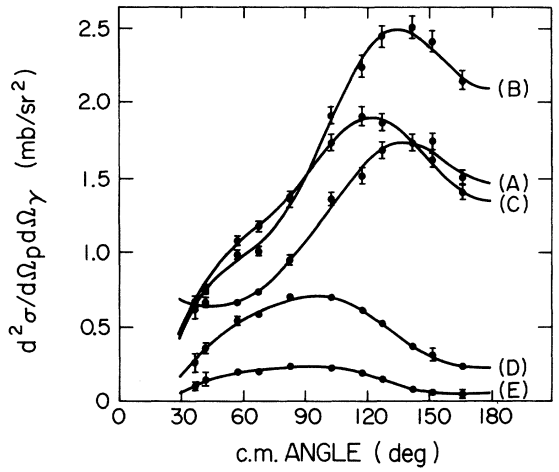

FIG. 2. The ^{28}Si$(p, p'\gamma)^{28}$Si (2^+, 1.78 MeV) angular correlations in the spin-flip geometry over the E_p=4.23 MeV resonance in ^{29}P. Curve A corresponds to a bombarding energy of 4.225 MeV; B to 4.230 MeV; C to 4.240 MeV; D to 4.250 MeV; and E to 4.275 MeV. The solid curve is a least-squares fit to the data, for each energy.

geometry we are looking for the probability of detecting γ rays emitted along the z axis, where the z axis is defined perpendicular to the reaction plane, in coincidence with the inelastically scattered protons leaving ^{28}Si in its first-excited 2^+ state at 1.78 MeV.

A shielded 10.2×12.7 cm NaI(Tl) γ-ray detector was mounted in a special lid in our Ortec 43.2 cm scattering chamber. Six solid-state detectors were positioned in the chamber in the same geometry as was used for the angular-distribution experiments. For these measurements the target thickness was 65 μg/cm^2. Coincidences were recorded between the γ-ray detector and the six proton detectors simultaneously. Twelve coincident γ-ray spectra were stored in the computer; six spectra with real plus accidental coincidences and six with accidental coincidences alone. At any one bombarding energy a total of 24 coincident spectra were collected corresponding to 12 proton detector angles. Both the proton and γ-ray signals were examined for pulse pileup and the data so corrected. The proton bombarding energy was varied from 3.0 to 5.0 MeV and a total of 53 spin-flip correlations were measured. The average time required to perform one complete angular correlation at one energy was three hours. The spin-flip correlations were converted to absolute cross sections with an over-all uncertainty of ±6%; most of the uncertainty being due to target thickness nonuniformities, uncertainties in peak-area extraction, and uncertainties in the determination of the absolute efficiency of the γ-ray detector. Finally, the data were corrected for the finite solid angle of the γ-ray detector.

Five spin-flip angular correlations measured over the 4.2 MeV $5/2^+$ resonance are shown in Fig. 2. The solid curves shown in the figure are the least-squares fit to the data in terms of the $\cos\kappa\phi$ functions for κ both even and odd. Coefficients of the cosine functions were extracted and plotted as a function of proton bombarding energy for additional data from which resonant parameters could be determined.

For the third experimental geometry in this analysis, data were used from the proton-γ-ray angular correlations in the Goldfarb-Seyler geometry reported by Gearhart *et al.*[1] These correlations were converted to absolute cross sections with an over-all uncertainty of ±6%.

IV. DATA ANALYSIS

After the data had been converted to absolute cross sections and the least-square fits obtained for the expansion functions corresponding to each of the three geometries, the expansion coefficients were stored on magnetic disks so that the energy variations of the expansion coefficient could be recalled and displayed for view on our off-line storage oscilloscope. The technique for determining the resonant decay parameters was to calculate theoretically the values of the expansion coefficients, as shown in Sec. II, for a trial set of resonant parameters, i.e., decay widths and phases.

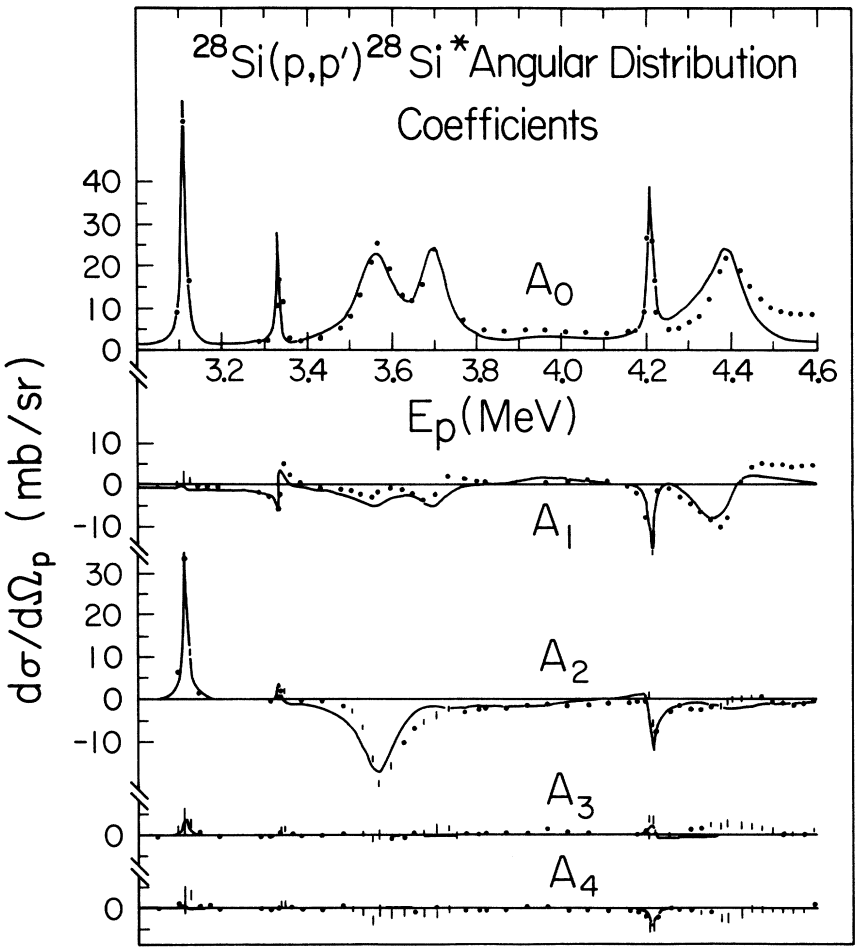

FIG. 3. The ^{28}Si$(p, p')^{28}$Si* (2^+, 1.78 MeV) inelastic angular distributions from a bombarding energy of 3.0 to 4.6 MeV. At each bombarding energy the coefficients of the angular distributions were extracted from Eq. (2) and plotted as a function of energy. The solid curve is a theoretical fit to the experimental coefficients using the parameters of Table I.

The trial set of parameters was chosen initially to consist of only the lowest possible l value allowed in the decay. Higher l-value partial waves were added only when needed to improve the visual fits. The energy variations of the calculated coefficients were then displayed on our storage scope as an overlay on the experimental data. For a trial set of input decay parameters, the results for each of the three geometries were visually examined in turn. In practice we were aided by the fact that for each geometry, certain expansion coefficients were more sensitive to certain decay channels than to others. Consequently, the iteration of parameters went fairly quickly until a best visual fit of the theoretical calculations to the data was obtained.

As an example of the calculations performed to evaluate the expansion coefficients for say the angular distributions, Eq. (1) was programmed in accordance with the expansion $d\sigma/d\Omega_p = \sum_k A_k P_k(\cos\theta)$. The expansion coefficients for this geometry could then be expressed as

$$A_k(E) = \sum_{J_b \pi_b J_{b'} \pi_{b'}} \sum_{j_2 j_2'} B(\alpha) \frac{F_1 + F_2 E + F_3 E^2}{[(E - E_b)^2 + \frac{1}{4}\Gamma_b^2][(E - E_{b'})^2 + \frac{1}{4}\Gamma_{b'}^2] E},$$

where

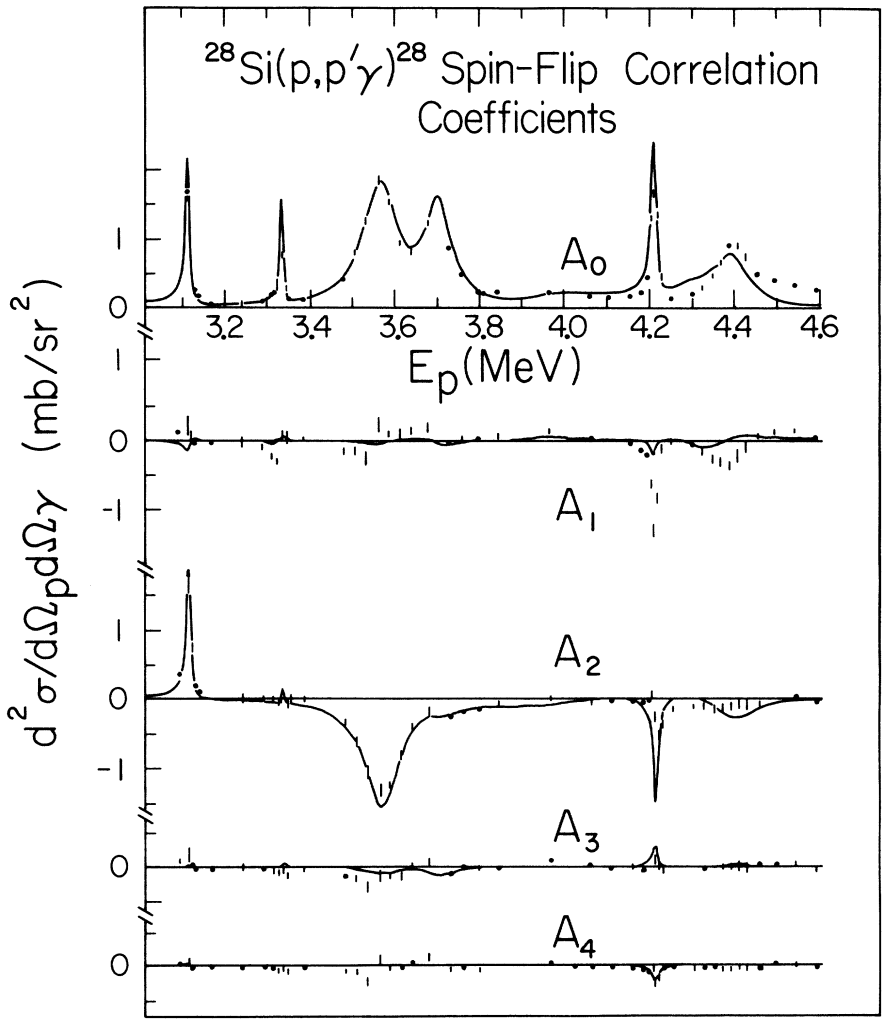

FIG. 4. The ^{28}Si$(p, p'\gamma)^{28}$Si* (2^+, 1.78 MeV) angular correlations in the spin-flip geometry. At each bombarding energy the coefficients were extracted from Eq. (3) and plotted as a function of energy. The solid curve is a theoretical fit to the experimental coefficients using the parameters of Table I.

$$B(\alpha) = \sum_{\substack{l_1 l_1' \\ l_2 l_2'}} (\text{const}) \hat{J}_b^3 \hat{J}_{b'}^3 (-)^{2J_{b'}-1} \hat{l}_1 \hat{l}_1' \hat{l}_2 \hat{l}_2' \hat{j}_2 \hat{j}_2' (l_1 0 l_1 0 | k0) W(l_1 l_1' J_b J_{b'}; k\tfrac{1}{2})$$

$$\times (l_2' 0 l_2 0 | k0) W(l_2' l_2 j_2' j_2; k\tfrac{1}{2}) W(J_b J_{b'} J_b J_{b'}; k0) W(J_b J_{b'} j_2 j_2'; k2)$$

and

$$F_1 = (\Gamma_{j_1} \Gamma_{j_1'} \Gamma_{j_2} \Gamma_{j_2'})^{1/2} \{ [E_b E_{b'} + \tfrac{1}{4}(\Gamma_b \Gamma_{b'})] \cos(\phi_{j_1} + \phi_{j_2} - \phi_{j_1'} - \phi_{j_2'})$$

$$+ [\tfrac{1}{2}(\Gamma_{b'} E_b) - \tfrac{1}{2}(\Gamma_b E_{b'})] \sin(\phi_{j_1} + \phi_{j_2} - \phi_{j_1'} - \phi_{j_2'}) \},$$

and F_2 and F_3 are similar functions of the same variables as F_1. The expansion coefficients were formulated in this manner for ease of programming and speed of calculations. The results of the analysis and the comparison with the experimental coefficients are shown in Figs. 3, 4, and 5 for the angular distribution, spin-flip correlation, and Goldfarb-Seyler geometries, respectively. All en-

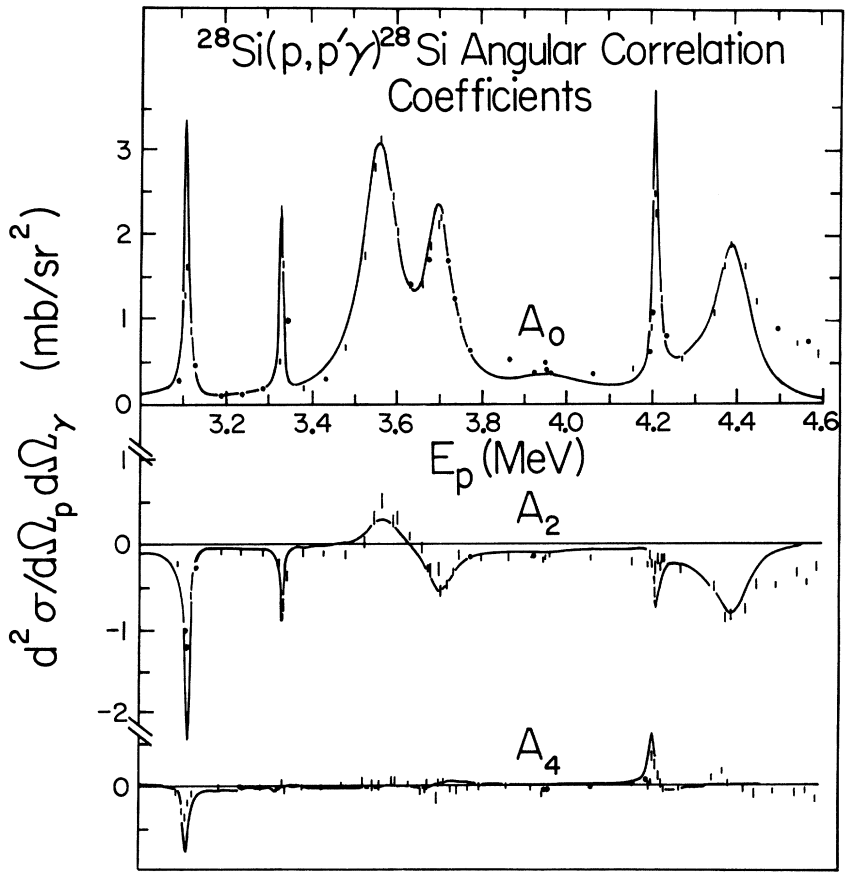

FIG. 5. The ^{28}Si$(p, p'\gamma)^{28}$Si* (2^+, 1.78 MeV) angular correlations measured in the Goldfarb-Seyler geometry. At each bombarding energy the coefficients were extracted from Eq. (4) and plotted as a function of bombarding energy. The solid curve is a theoretical fit to the experimental coefficients using the parameters of Table I.

ergies are in lab coordinates while the cross sections shown in the three figures are in c.m. coordinates. The final set of partial decay widths and phases corresponding to the best visual fit are shown in Table I.

It is difficult to make an accurate determination of the uncertainties associated with the assigned partial widths and phases. Due to the large number of these parameters, it was felt that a multiparameter χ^2 fit to the data would be impractical. Instead we have varied a few of the parameters in turn and attempted to observe at which point the visual fits appeared to worsen. Typically some of these widths could vary by ±20% before an observable change is seen; for other phases as little as ±10% or as great as ±100% variation could occur before seeing an observable change. In general, of course, the large uncertainties of ±100% occurred for those partial widths of the smallest relative magnitude.

Up to a bombarding energy of 4.78 MeV, the only energetically allowed particle decay channels are the elastic channel and the inelastic proton decay channel to the first excited 2^+ state in ^{28}Si at 1.78 MeV. For the resonances studied up to a bombarding energy of 4.78 MeV, the background in the excitation curve seems to be due primarily to the tails of the resonances themselves. See Fig. 1 of Ref. 1. Typical peak-to-background ratios in this energy region vary from 5 : 1 to about 20 : 1. Consequently, for our analyses of the resonances in this energy region we made the assumption that the resonances interfered primarily only with each other. An exception was made for two broad spin-1/2 resonances and one broad spin-3/2 resonance known to be located outside this excitation region but whose influence in this region was important because of the broad widths of the resonances.

Above about 4.8 MeV bombarding energy, not only does a second inelastic decay channel open but the background under the resonances above this energy increases markedly so that the peak-

TABLE I. Resonance parameters for states in ^{29}P.

Input parameters [a]					Decay widths [Γ_{lj} (keV)] and phases [b] [ϕ_j (deg)]													
E_p (MeV lab)	E_x (MeV)	J^π	Γ (keV)	Γ_p (keV)	$s_{1/2}$	$\phi_{1/2}$	$p_{1/2}$	$\phi_{1/2}$	$p_{3/2}$	$\phi_{3/2}$	$d_{3/2}$	$\phi_{3/2}$	$d_{5/2}$	$\phi_{5/2}$	$f_{5/2}$	$\phi_{5/2}$	$f_{7/2}$	$\phi_{7/2}$
2.88	5.52	$\frac{1}{2}^-$	400	395					5	110								
3.10	5.74	$\frac{7}{2}^-$	13.6	3.9					9.7	−130								
3.33	5.96	$\frac{3}{2}^+$	8.4	6.4	2	−95					0.01	110	0.01	110				
3.57	6.19	$\frac{3}{2}^-$	98	20			11	−120	65	−120					0.9	60	0.2	−120
3.71	6.33	$\frac{3}{2}^+$	74	18	55.5	−80					0.4	−80	0.3	100				
3.98	6.58	$\frac{1}{2}^+$	200	189							10	−160	1	180				
4.23	6.83	$\frac{5}{2}^+$	15	5	7	−110					2	95	1	30				
4.36	6.96	$\frac{1}{2}^+$	120	112							7	0	1	100				
4.43	7.02	$\frac{3}{2}^-$	100	30			25	130	45	−70								
4.88	7.46	$\frac{5}{2}^-$	8.6	3.6			4.5	0	0.5	0								
4.95	7.52	$(\frac{1}{2}^-)$	7	3					4	0								
5.07	7.64	$\frac{1}{2}^+$	240	180							30	110	30	−20				
5.19	7.76	$(\frac{3}{2}^+)$	8	2	6	180												
5.44	8.01	$\frac{3}{2}^-$	130	80			25	130	25	−70								

[a] Input parameters obtained from Refs. 1, 3, 4, and 5 or as described in text.
[b] All output phases measured relative to an input phase of 0°.

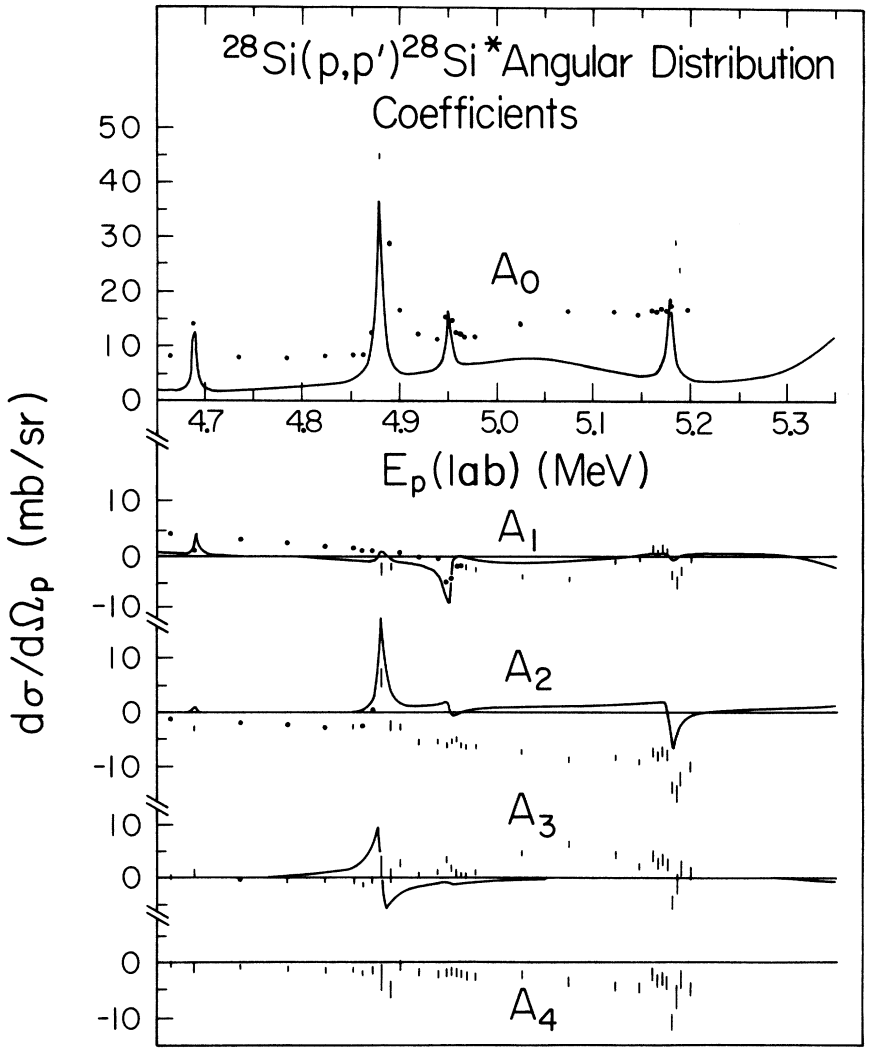

FIG. 6. The ^{28}Si(p, p')^{28}Si* (2^+, 1.78 MeV) inelastic angular distributions from a bombarding energy of 4.6 to 5.2 MeV. See caption of Fig. 3.

to-background ratio for the three resonances studied was on the order of 1 : 1. It appears likely that most of this background is due to the tails of the large number of more highly excited resonances and whose parameters are for the most part not known. Although the background is probably due to the tails of a large number of resonances, it does not approach a statistically large number since we are still able to observe interference terms in the odd coefficients. Consequently, for the region above 4.8 MeV bombarding energy, only approximate fits to the data were possible. The results of these partial fits are contained in Figs. 6 and 7 and in Table I.

V. RESULTS

A. 3.10 MeV resonance

The original spin assignment of $5/2^-$ for this resonance was made by Vorona, Olness, Haeberli, and Lewis[3] and confirmed by Belote, Kashy, and Risser.[4] Both experiments involved measurements of the differential elastic scattering cross section and were consistent only with an f-wave, $j = 5/2^-$ or $7/2^-$, assignment. In addition to the elastic scattering measurements, Belote *et al.* measured a single angular distribution of inelastically scattered protons at the peak of the resonance and from these data ruled out a $7/2^-$ assignment.

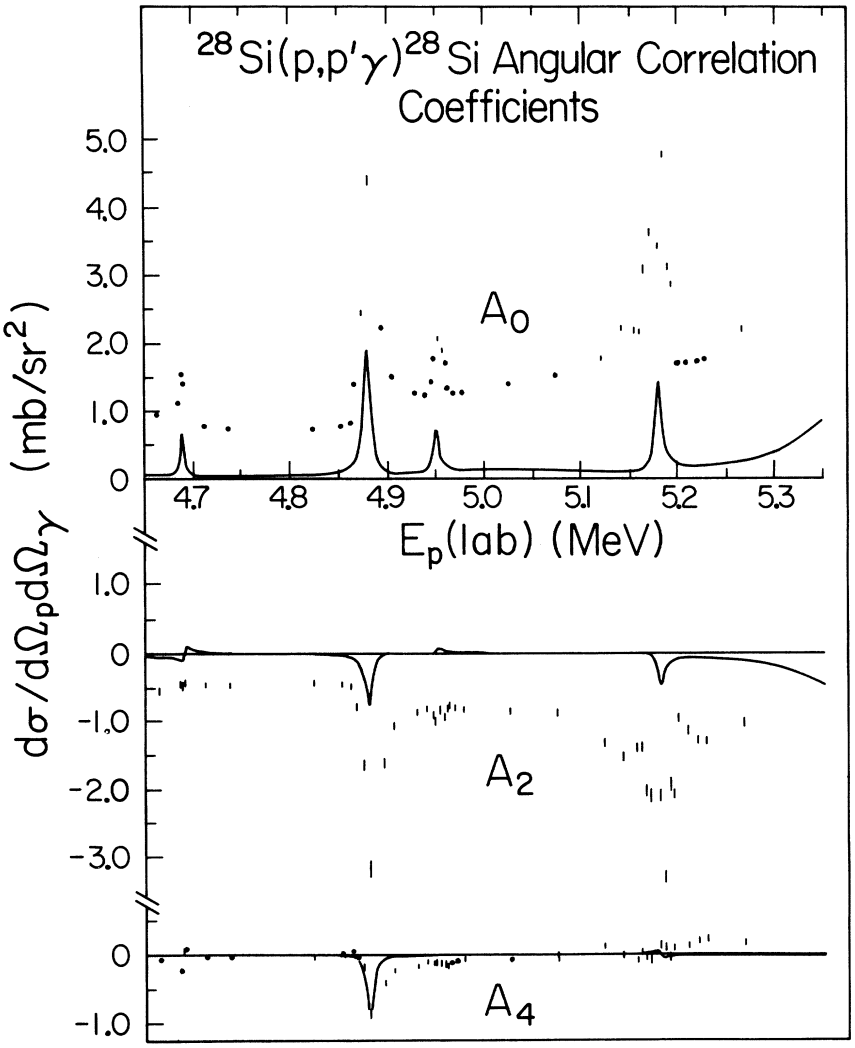

FIG. 7. The ^{28}Si($p, p'\gamma$)^{28}Si* (2^+, 1.78 MeV) angular correlations in the Goldfarb-Seyler geometry measured from a bombarding energy of 4.6 to 5.3 MeV. See caption of Fig. 5.

Gearhart *et al.*[1] determined only that the spin of this resonance was 5/2 or greater. For our present measurements, it was possible to obtain equally good fits to the angular distributions for either a $5/2^-$ or $7/2^-$ spin, but with different values for the decay widths.

In order to obtain a definitive spin assignment for this state, an elastic scattering measurement was performed over this resonance using the recently developed polarized proton beam of this laboratory. The result of this measurement, reported by McEver, Arnold, and Donoghue,[9] was that the spin of the state was $7/2^-$. Consequently, this spin assignment was the one used in the partial width analysis.

The fits to the data over this resonance, shown in Figs. 3–5, were obtained by assigning the total strength of the inelastic partial proton decay width to lie in the $p_{3/2}$ channel. The presence of the odd A_3 coefficient appears to be due to the interference of this state with both of the nearby $3/2^+$ resonances at $E_p = 3.33$ and 3.71 MeV.

B. 3.33 MeV resonance

The appearance of a nonzero A_1 coefficient in both the proton angular distributions and spin-flip correlations indicates that this $3/2^+$ resonance is interfering with other resonances of opposite parity. The contribution to this interference term from the $7/2^-$ resonance at 3.10 MeV is very small due to the narrow energy width of the 3.10 MeV state. The dominant contributions to the interfer-

ence terms comes from the broad (400 keV) $1/2^-$ resonance at 2.88 MeV and from the $3/2^-$ resonance at 3.57 MeV. In order to obtain the best visual fit to all three geometries, it was necessary to include some $l=2$ channel decay as well as $l=0$. Although the measured contribution of the $d_{5/2}$ decay is only 1/2% of the $s_{1/2}$ contribution, penetrability effects change the $d_{5/2}$ reduced width to 8% of the $s_{1/2}$ reduced width.

C. 3.57 and 3.71 MeV doublet

While there is agreement in the literature as to the $3/2^-$ spin and parity of the 3.57 MeV member of this overlapping doublet, contradicting spin and parity assignments are reported for the 3.71 MeV resonance. Vorona *et al.*[3] report the spin and parity of the 3.71 MeV resonance as $3/2^+$, Belote *et al.*[4] report the resonance as $1/2^-$, and Soroka and Pucherov[10] report the resonance as $1/2^-$. The angular-correlation measurements in the Goldfarb-Seyler geometry reported by Gearhart *et al.*[1] and shown in Fig. 5 make a definite 3/2 spin assignment to the 3.71 MeV resonance.

The results of the proton angular distribution and spin-flip angular-correlation measurements shown in Figs. 3 and 4 show interference in the A_1 coefficient, and for the A_3 coefficient in the spin-flip measurements. We can account for this interference only by having the two states interfere with one another indicating that they must have opposite parity. The recent polarization measurements of McEver *et al.*[9] also verify that the spin of the 3.71 MeV resonance is $3/2^+$. Considering all the evidence, there appears to be little doubt that the spin and parity of the 3.71 MeV resonances is $3/2^+$.

The fits to the three geometries of Figs. 3, 4, and 5 were made on the basis of the above spin assignments. Reasonably good fits were obtained for the three geometries although nonzero values of the inelastic partial decay widths corresponding to higher l values than the lowest possible ones were necessary to obtain the fits. For the 3.57 MeV resonance, both p and f waves were required for the fit; for the 3.71 MeV resonance, both s and d waves were required.

D. 3.98 MeV resonance

Belote *et al.*[4] reported the presence of a broad 200 keV $1/2^+$ resonance which appeared strongly in the elastic channel but only weakly, if at all, in the inelastic proton channel. It was difficult to tell from observation as to whether the actual yield observed in the inelastic cross section over the energy range of this resonance was due to some contribution from the $1/2^+$ resonance or was merely due to the tails of higher-energy resonances. However, we found it necessary to include approximately a 7% inelastic contribution in order to account for interference in some of the coefficients of nearby resonances. The assumed amount of inelastic contribution also reasonably reproduced the cross section in the A_0 coefficients of all three geometries.

E. 4.23 MeV resonance

The narrow resonance at $E_p=4.23$ MeV was reported by Belote *et al.*[4] as an $l=2$, $j=3/2$ or $5/2$, resonance. They concluded from a study of a single angular distribution of inelastically scattered protons on resonance that the state was $3/2^+$. As with other resonances we have examined, a single angular distribution measured on resonance is usually not sufficient for a unique spin assignment. Rather, we have found it necessary to measure angular distributions at a number of energies across the resonance in order to more explicitly show the energy variations of the measured parameters. The angular-correlation measurements reported by Gearhart *et al.*[1] and shown here in Fig. 5 are consistent only with a $j=5/2^+$ assignment assuming an $l=2$ transfer in the elastic channel. The presence of an A_4 coefficient in both the angular distribution and spin-flip correlation measurements, shown in Figs. 3 and 4, respectively, confirms the $5/2^+$ assignment of Gearhart *et al.* Due to the limitation on the complexity of the distributions ($k_{\max} \leq 2J_b$), as given in Eq. (2), a resonance spin of 3/2 would limit the complexity of the angular distribution to the maximum of an A_3 coefficient.

The fits shown in Figs. 3–5 include both s and d waves in the exit channel decays, with the d-wave channel containing approximately 30% of the inelastic decay strength. Interference between the 4.23 MeV resonance and the $3/2^-$ resonance at 4.43 MeV gives rise to both an A_1 and A_3 coefficient for the angular distributions and the spin-flip correlations.

In order to obtain the fits observed in Figs. 3–5, it was found necessary to increase the total width of the resonance from the 5.4 keV value reported by Belote *et al.* to the value of 15 keV, with a ratio of Γ_p/Γ of 0.33 rather than the value of 0.6. It is unlikely that this discrepancy is due to target thickness effects since our target thickness and that of Belote *et al.* are approximately the same, 3–4 keV. This is the only resonance of those studied whose total width and Γ_p/Γ ratio differed significantly from those reported by Belote *et al.*

F. 4.36 MeV resonance

Just as in the case of the 3.98 MeV resonance, the broad 120 keV $1/2^+$ resonance reported by

Belote *et al.* appears to have little observable strength in the inelastic proton decay channel. However, as in the case of the 3.98 MeV resonance, we have found it necessary to include some strength in the $d_{3/2}$ and $d_{5/2}$ inelastic decay channels, in order to fit the A_1 interference term observed at the 4.43 MeV resonance which overlaps the 4.36 MeV resonance.

G. 4.43 MeV resonance

The two broad resonances at 4.36 and 4.43 MeV with reported total widths of 120 and 100 keV, respectively, overlap strongly in the elastic channel, but only the 4.43 MeV resonance appears to have an appreciable strength in the inelastic proton channel. (As was pointed out in Sec. V F, the 4.36 MeV resonance does appear to have some strength in the inelastic channel.) Belote *et al.* report that the results of their elastic scattering cross section data restrict the possible assignments of this resonance as being either $1/2^-$ or $3/2^-$. Their measurement of a single inelastic scattering angular distribution on resonance showed a small A_1 coefficient. The results of both their elastic and inelastic scattering data lead them to a $1/2^-$ assignment for the 4.43 MeV resonance. However, the angular-correlation results reported by Gearhart *et al.* and shown in Fig. 5 are consistent only with a 3/2 spin assignment for the 4.43 MeV resonance. This conclusion results from the presence of a strong A_2 coefficient in the angular-correlation measurements which rule out a 1/2 spin assignment.

The results of the angular distribution and spin-flip correlation experiments show some interesting results. For both experiments, the odd A_1 coefficient measured across the broad resonance shows a large negative value on the low-energy side of the peak and a positive value on the high-energy side of the peak. Five of the angular distributions across this resonance are shown in Fig. 8. Since Belote *et al.* measured their single inelastic angular distribution on the resonance peak, they observed only a small A_1 coefficient since the A_1 coefficient is passing through zero near the peak. The very large values of the A_1 coefficient across this resonance indicates a strong interference of the 4.43 MeV resonance with positive parity resonances. In order to obtain the fits shown in Figs. 4 and 5, it was found necessary to assign a $3/2^-$ value to the resonance and to include interference from the overlapping $1/2^+$ resonance at 4.36 MeV and the broad $1/2^+$ resonance at 5.07 MeV reported by Brenner, Hoogenboom, and Kashy.[5] The negative portion of the A_1 coefficient appears to be due primarily to interference with the 4.36 MeV state whereas the positive portion of the A_1 coefficient appears to be due to interference with the 5.07 MeV resonance.

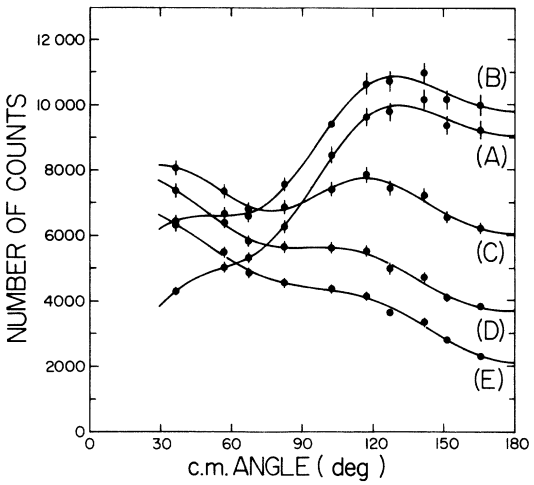

FIG. 8. The ^{28}Si$(p, p')^{28}$Si* (2^+, 1.78 MeV) inelastic angular distributions over the 4.43 MeV resonance in ^{29}P. Curve A corresponds to a bombarding energy of 4.395 MeV; B to 4.410 MeV; C to 4.45 MeV; D to 4.470 MeV; and E to 4.500 MeV. The solid curves are least-squares fits to the experimental data at each energy.

The appearance of a nonzero A_3 coefficient over this resonance is also of some interest. A nonzero value of this coefficient cannot be due to interference with a $1/2^+$ resonance such as was the case for the A_1 coefficient. The A_3 coefficient must be due to interference with positive parity resonances of spin $\geq 3/2$. [See Eq. (2).] The interference represented in this coefficient could be due to nearby narrow resonances, such as the $5/2^+$ resonance at 4.23 MeV, or to broad resonances somewhat further away in energy. The maximum contribution to the A_3 coefficient that we were able to obtain from interference with the $5/2^+$ resonance at 4.23 MeV was an order of magnitude smaller than the measured values. Consequently we searched the literature for higher-energy positive parity states having sufficient width and with spin $\geq 3/2$. The only possible candidate we could find in the literature was a broad 130 keV $1/2^-$ or $3/2^-$ resonance at $E_p = 5.44$ MeV reported by Brenner *et al.* but due to its negative parity, this state could not produce interference in the odd A_3 coefficient. By assuming the resonance at 5.44 MeV to have a positive parity and a spin of 3/2, we were able to generate a positive A_3 coefficient over the 4.43 MeV resonance which reasonably fit the data in Fig. 4. However, we do not feel that this one piece of data is sufficient evidence for changing the parity assignment made by Brenner *et al*. Consequently, the fits shown in Figs. 4 and

TABLE II. Reduced widths for proton decay channels of resonances in ^{29}P. The reduced widths $\theta_{lj}^2=(\mu a^2)/(\hbar^2)\gamma_{lj}^2$ are reported in units of $\hbar^2/\mu a^2$, where μ is the reduced mass and $a=5.7$ fm.

E_p (MeV lab)	E_x (MeV)	J^π	Reduced widths θ_{lj}^2 $s_{1/2}$	$p_{1/2}$	$p_{3/2}$	$d_{3/2}$	$d_{5/2}$	$f_{5/2}$	$f_{7/2}$
2.88	5.52	$\frac{1}{2}^-$			0.28				
3.10	5.74	$\frac{7}{2}^-$			0.17				
3.33	5.96	$\frac{3}{2}^+$	0.005			0.0004	0.0004		
3.57	6.19	$\frac{3}{2}^-$		0.047				0.26	0.06
3.71	6.33	$\frac{3}{2}^+$	0.079			0.008	0.006		
3.98	6.58	$\frac{1}{2}^+$				0.11	0.010		
4.23	6.83	$\frac{5}{2}^+$	0.005			0.010	0.005		
4.36	6.96	$\frac{1}{2}^+$				0.025	0.003		
4.43	7.02	$\frac{3}{2}^-$		0.026	0.048				
4.88	7.46	$\frac{5}{2}^-$		0.002	0.0003				
4.95	7.52	$(\frac{1}{2}^-)$			0.002				
5.07	7.64	$\frac{1}{2}^+$				0.053	0.053		
5.19	7.76	$(\frac{3}{2}^+)$	0.002						
5.44	8.01	$\frac{3}{2}^-$		0.014	0.014				

5 are made assuming that the resonance at 5.44 MeV was a negative parity resonance as reported.

H. 3.97 and 4.69 MeV resonances

The two very narrow resonances $\Gamma \leq 3$ keV at 3.97 and 4.69 MeV bombarding energy were erroneously reported in Ref. 1 as having been seen for the first time. Actually, the 3.97 MeV resonance was first reported by Willard, Bair, Cohn and Kington[11] in the ^{28}Si$(p, p'\gamma)^{28}$Si reaction, and the 4.69 MeV resonance was also observed by the same group.[12] In the experiments reported here, we were unable to add any further information as to the structure of these two resonances.

I. Resonances between a bombarding energy of 4.7 and 5.2 MeV

At a bombarding energy of about 4.7 MeV, the yield in the inelastic proton decay channel increases sharply. The inelastic yield curve is shown as Fig. 1 in Ref. 1. The effect can also be observed in the A_0 and A_2 coefficients in Figs. 6 and 7. We attribute this background to the tails of higher excitation-energy resonances of generally unknown properties. Consequently, our attempts to determine the decay parameters of the resonances in this energy region, which reside upon this background, are frustrated by the fact that the odd expansion coefficients are dominated by the interference with the background. For this reason the more tedious spin-flip correlation measurements were not performed over this energy region. The results of the angular-correlation measurements in the Goldfarb-Seyler geometry and the inelastic angular distribution measurements are shown in Figs. 6 and 7, respectively. The general shape of the energy dependence of the even coefficients can be reproduced but not a detailed fit to the data. The calculated structure in the odd coefficients is probably spurious since we are unable to account for the dominant interference with the background. Although the partial decay widths and phases which represent the calculated curves in Fig. 6 and 7 are included in Table II, we do not have the same confidence in these values as we do for the values at the lower energies primarily because we are unable to take into detailed account the interference of these resonances with the background.

VI. DISCUSSION

Since we did not perform a search on partial decay widths and phases in fitting to the experimental coefficients, the question arises as to whether

the fits reported are unique. In order to test the uniqueness of the fits, we performed a number of tests. For a particular resonance in one of the geometries, say the inelastic scattering angular distributions, we attempted to find sets of partial waves and phases that visually gave a reasonable fit to the experimental coefficients. For some of the resonances, more than one set of widths and phases gave reasonable visual fits. However, when these different sets of widths and phases were used to calculate theoretical coefficients for the other geometries, i.e., the Goldfarb-Seyler and spin-flip geometries, only one of the sets gave reasonable fits to the coefficients in the other geometries. Although the tests we performed were not exhaustive, we believe that the partial decay widths and phases reported are a unique set.

The reduced widths γ_{lj}^2 can be calculated from the experimental partial widths through the approximate relation[13] $\gamma_{lj}^2 = \Gamma_{lj}/[2P_l(E_p)]$ where $P_l(E_p)$ is the penetrability factor. Since the quantities γ_{lj}^2 are independent of the energy of the incident particle and depend upon the nuclear wave function which describes the resonances states, nuclear model predictions can be compared to the determined quantities. Model calculations of ^{29}P for energy level predictions have not as yet been extended to the excitation energy region we have studied. Therefore, we did not attempt to apply any nuclear structure model in order to calculate the reduced widths. The experimentally determined reduced widths in units of $\hbar^2/\mu a^2$ are shown in Table II.

The authors wish to thank J. F. Morgan, R. G. Seyler, and W. S. McEver for many fruitful discussions and L. A. Alexander for his help in programming.

---

†Work supported in part by the National Science Foundation.

*Present address: IBM Corporation, 140 E. Town St., Columbus, Ohio 43215.

[1]N. L. Gearhart, H. J. Hausman, J. F. Morgan, G. A. Norton, and N. Tsoupas, Phys. Rev. C 10, 1739 (1974).
[2]L. J. B. Goldfarb and R. G. Seyler, Phys. Lett. 28B, 15 (1968).
[3]J. Vorona, J. W. Olness, W. Haeberli, and H. W. Lewis, Phys. Rev. 116, 1563 (1959).
[4]T. A. Belote, E. Kashy, and J. R. Risser, Phys. Rev. 122, 920 (1961).
[5]M. W. Brenner, A. M. Hoogenboom, and E. Kashy, Phys. Rev. 127, 947 (1962).
[6]G. R. Satchler, Ann. Phys. (N.Y.) 3, 278 (1958).
[7]S. Devons and L. J. B. Goldfarb, in *Handbuch der Physik, Nuclear Reactions*, edited by S. Flügge (Springer-Verlag, Berlin, 1957), Vol XLII, Part III, p. 362.
[8]F. H. Schmidt, R. E. Brown, J. B. Gerhart, and W. A. Kolasinsky, Nucl. Phys. 52, 353 (1964).
[9]W. S. McEver, L. G. Arnold, and T. R. Donoghue (unpublished).
[10]V. I. Soroka and N. N. Pucherov, Yad. Fiz. 9, 1159 (1969) [Sov. J. Nucl. Phys. 9, 677 (1969)].
[11]H. B. Willard, J. K. Bair, H. O. Cohn, and J. O. Kington, Bull. Am. Phys. Soc. 1, 264 (1956).
[12]J. K. Bair (private communication).
[13]H. E. Gove, *Nuclear Reactions*, edited by P. M. Endt and M. Demeur (North-Holland, Amsterdam, 1959), Vol. I, Chap. VI.